Available online at www.sciencedirect.com
ScienceDirect
Ceramics International 35 (2009) 1909–1917
CERAMICS INTERNATIONAL
www.elsevier.com/locate/ceramint

Sintering and mechanical properties of tricalcium phosphate–fluorapatite composites

Nadhem Bouslama, Foued Ben Ayed *, Jamel Bouaziz

Laboratory of Industrial Chemistry, National School of Engineering, BP 1173, 3038 Sfax, Tunisia

Received 26 June 2008; received in revised form 23 August 2008; accepted 20 October 2008
Available online 21 November 2008

Abstract

Tricalcium phosphate and synthesized fluorapatite powder were mixed in order to elaborate biphasic ceramics composites. The effect of fluorapatite addition on the densification and the mechanical properties of tricalcium phosphate were measured with the change in composition and microstructure of the bioceramic. The Brazilian test was used to measure the mechanical resistance of the tricalcium phosphate–26.52 wt% fluorapatite composites. The densification and rupture strength increase versus sintering temperature. The composites have a good sinterability and rupture strength in temperature ranging between 1300 and 1400 °C. Thus, the densification ultimate was obtained at 1350 °C and the mechanical resistance optimum reached 9.6 MPa at 1400 °C. Above 1400 °C, the densification and the mechanical properties were hindered by the allotropic transformation of tricalcium phosphate, grain growth and the formation of both intragranular porosity and many cracks. The ^{31}P magic angle spinning nuclear magnetic resonance analysis of composites reveals the presence of tetrahedral P sites.

Keywords: A. Sintering; B. Composites; C. Mechanical properties; E. Biomedical applications; Bioceramics

1. Introduction

Hydroxyapatite (Hap) and β tricalcium phosphate (β-TCP) are the most commonly used bioceramics due to their biocompatibility and bioactivity/restorability that can be modeled under an appropriate shape and size [1–10]. These bioceramics have a wide range of potential applications for bone substitutes either in the form of dense or porous parts. These bioceramics favour bone reconstruction, thanks to height restorability as β-TCP and good osteoconductivity as Hap [3]. For many years, the synthesized calcium phosphates have been used clinically to repair bone defects [1–4]. But the use of its bioceramic was always restricted because of its fragility and the weak rupture resistance [3,5]. Hence, there was a need for maximizing the mechanical properties of tricalcium phosphate suitable for biomedical applications.

Among these materials fluorapatite (Fap) has excellent biocompatibility with the adjacent hard tissue [11–18]. The Fap was known to have a high chemical stability of Hap [2,3]. Moreover, Fap has a potential advantage by comparison with Hap according to its higher thermal stability and aptitude to delay caries process without the biocompatibility degradation [11–18]. In the context, this study was undertaken to evaluate the sintering and mechanical properties behaviour of the commercial tricalcium phosphate (β-CTCP)–fluorapatite (Fap) composites. The aim of this work is to prepare biphasic calcium phosphates composites sintered at various temperatures (1100–1450 °C) for 1 h. Fap has been used with a fixed 26.52 wt% amount because the human bone contains 1 wt% of fluorine approximately [17,18]. The samples were characterized by magic angle spinning nuclear magnetic resonance (MAS-NMR), scanning electron microscopy (SEM), infrared spectrometric (IR), dilatometry, X-ray diffraction (XRD) and differential thermal analysis (DTA).

2. Materials and methods

2.1. Preparation of powder and ceramic specimens

In this study the materials to be used are commercial tricalcium phosphate (Fluka) and synthesized fluorapatite. The Fap powder was synthesized by the precipitation method [13].

* Corresponding author. Tel.: +216 98 252 033; fax: +216 74 676 908.
E-mail address: benayedfoued@yahoo.fr (F. Ben Ayed).

0272-8842/$34.00.
doi:10.1016/j.ceramint.2008.10.030

Then, a calcium nitrate ($Ca(NO_3)\cdot 4H_2O$, Merck) solution was slowly added to a boiling solution containing diammonium hydrogenophosphate ($(NH_4)_2HPO_4$, Merck) and ammonium fluorine (NH_4F, Merck), with continuous magnetic stirring. During the reaction, pH was adjusted to the same level (pH 8–9) by adding ammonia. The obtained precipitate was filtered and washed with deionised water; it was then dried at 70 °C for 12 h.

The approximate representatives Fap–β-CTCP were respectively, 26.52 wt%, 73.48 wt%. Estimated quantities of each powder were milled with absolute ethanol and treated by ultrasound machine for 15 min. The milled powder was dried at 120 °C in a steam room to remove the ethanol and produce a finely divided powder. Powder mixtures were moulded in a metal mould and uniaxially pressed at 150 MPa to form cylindrical compacts with a diameter of 20 mm and a thickness of about 6 mm. The green bodies were sintered at various temperatures (between 1050 and 1450 °C) for 1 h. The green compacts were sintered in a vertical resistance furnace (Pyrox 2408). The best holding time for obtaining the maximum densification is 1 h. The heating and cooling rates were 10 and 20 °C min^{-1}, respectively. The relative densities of the sintered bodies were calculated by the dimensions and weight. The relative error of densification and mechanical resistance values were 1% and 1 MPa, respectively.

2.2. Characterization methods of powder and ceramic specimens

The received powder was analyzed using X-ray diffraction (XRD). The X-rays have used the Seifert XRD 3000 TT diffractometer. The X radiance was produced by the use of CuK_α radiation (λ = 1.54056 Å). Also, the crystalline phases were identified by reference to the ICDD files. The powder was also submitted to infrared spectrometric (IR) analysis (Perkin-Elmer 783). ^{31}P Nuclear magnetic resonance (MAS-NMR) spectra were run on a Brucker 300WB spectrometer. The ^{31}P observational frequency was 121.49 MHz with 3.0 ms pulse duration, spin speed 8000 Hz and delay 1 s with 2048 scans. ^{31}P shift was given in parts per million (ppm) referenced to 85 wt% H_3PO_4. Different thermal analysis was carried out using about 30 mg of powder in helium (DTA; Model Setaram). The heating rate was 5 °C min^{-1}. Linear shrinkage was determined by dilatometry (Setaram TMA 92 dilatometer) using the same thermal cycle as the one used for DTA.

The particle size dimension of the powder was measured by means of Micromeritics Sedigraph 5000. The specific surface area (SSA) was measured by the BET method using azotes (N_2) as an adsorption gas (ASAP 2010) [19]. The main particle size (D_{BET}) was calculated by the assumption that the primary particles are spherical [14]:

$$D_{BET} = \frac{6}{S\rho} \quad (1)$$

where ρ is the theoretical density of β-CTCP (3.07 g cm^{-3}) or Fap (3.19 g cm^{-3}) and S is the SSA.

The microstructure of the sintered compacts was investigated by scanning electron microscopy (SEM Phillips XL 30) on sample-fractured surfaces.

Mechanical properties of the compacts were measured by Brazilian test. The optimum rupture strengths σ_r was offered by equation [16,20,21]:

$$\sigma_r = \frac{F}{S} = \frac{2F}{\Pi De} \quad (2)$$

where F is the tensile strength and D and e are the diameter and the thickness of the sample.

The Brazilian test was officially considered by the International Society for Rock Mechanics (ISRM) as a method for determining the tensile strength of rock materials [20]. The Brazilian test was also standardised by the American Society for testing materials (ASTM) to obtain the tensile strength of concrete materials [21].

3. Results and discussion

3.1. Characterization of the powder

The XRD pattern of the β-CTCP powder was reported in Fig. 1a. All the diffraction of tricalcium phosphate peaks corresponds to β-TCP (ICDD data file no. 09-0169) except two small peaks at 30,11° and 32,55° which are attributed to a pyrophosphate: β-$Ca_2P_2O_7$ (ICDD data file no. 09-0346). The XRD pattern obtained from Fap powder illustrated peaks relative to ICDD data file no. 15-876 (Fig. 1b).

Fig. 2 shows the FT-IR spectroscopic analysis of β-CTCP and Fap powders. The bands at 550, 606, 940, 970, 1020, 1116 and 1178 cm^{-1} and 468, 566, 606, 964, 1034, 1044 and 1076 cm^{-1} were characteristics of phosphate group of β-CTCP and Fap, respectively (Fig. 2a and b). The peaks at 940 and 1116 cm^{-1} are assigned to the stretching vibration of PO_4^{3-} ions and the peaks at 550 and 606 cm^{-1} are assigned to the deformation vibration of PO_4^{3-} ions. The bands at 3440 cm^{-1} were assigned to the adsorbed water molecule whereas the bands at 722 and 1194 cm^{-1} were assigned to the pyrophosphate (β-$Ca_2P_2O_7$) (Fig. 2a).

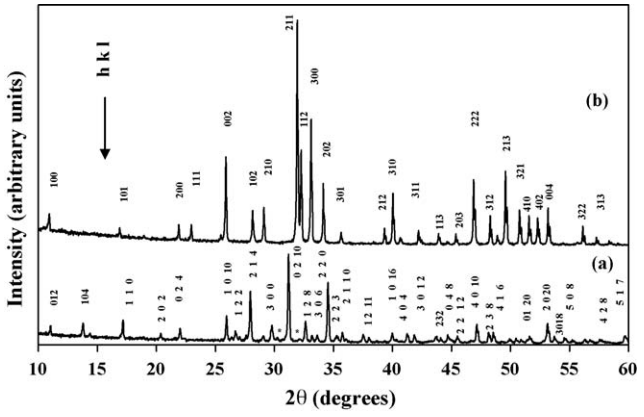

Fig. 1. XRD patterns of (a) β-CTCP powder, and (b) Fap powder (*β-$Ca_2P_2O_7$).

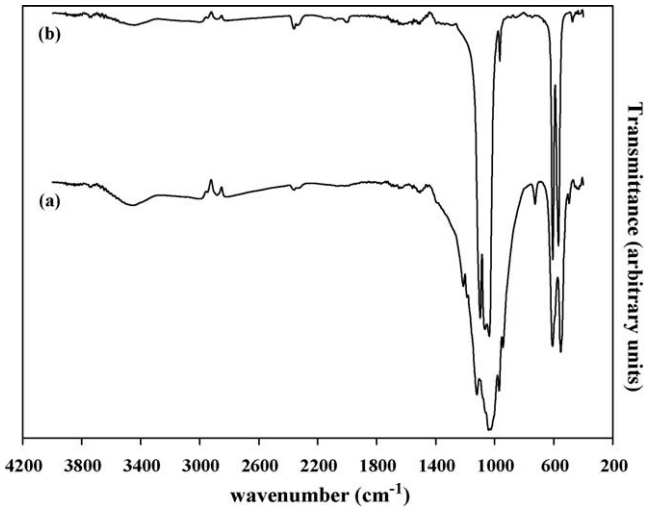

Fig. 2. IR spectra of (a) β-CTCP powder, and (b) Fap powder.

The ^{31}P MAS-NMR solid spectra of β-CTCP powder showed the resonance characteristic of the phosphate group (Fig. 3a). We have three peaks (4.64, 1.10 and 0.14 ppm) indicating the presence of three tetrahedral P sites (Q^1). Other peaks, at −8 ppm, reveal low quantity of pyrophosphate. This result confirms the XRD and IR analysis. Fig. 3b shows an intense peak at 2.80 ppm relative to the phosphorus of Fap which was assigned to tetrahedral sites (Q^1).

Fig. 4 shows the differential thermal analysis (DTA) curves of β-CTCP, Fap and β-CTCP–26.52 wt% Fap composites. The DTA thermogramme of β-CTCP (Fig. 4a) shows 3 peaks:

- The first endothermic peak, at 1278 °C, was linked to a binary peritectic between β-CTCP and pyrophosphate. The chemical reaction was illustrated in the following:

$$Ca_3(PO_4)_{2(s)} + Ca_2P_2O_{7(s)} \rightarrow Ca_3(PO_4)_{2(s)} + \text{liquid phase} \quad (3)$$

This result was similar to the previous reported by Destainville et al. [7].
- A second endothermic peak at 1290 °C showed the first allotropic transformation of the tricalcium phosphate: β to α.
- The last peak at 1464 °C is relative to the second allotropic transformation of tricalcium phosphate: α to α′.

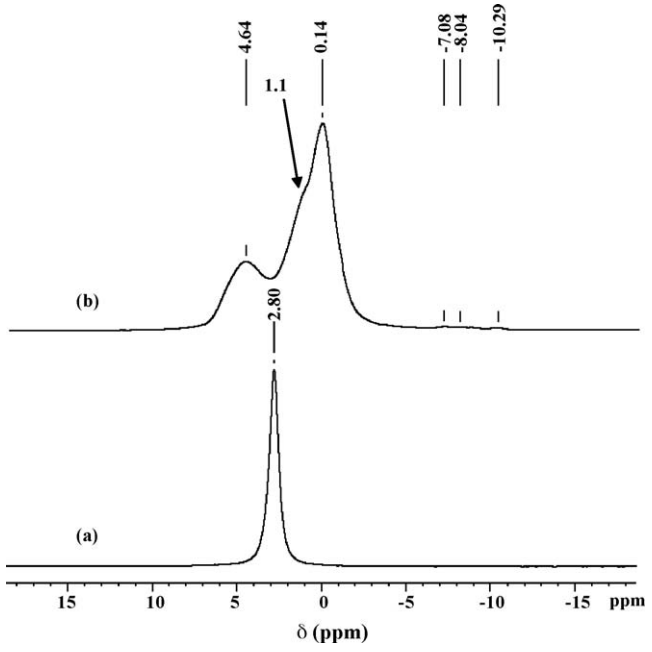

Fig. 3. ^{31}P MAS-NMR spectra of (a) Fap powder, and (b) β-CTCP powder.

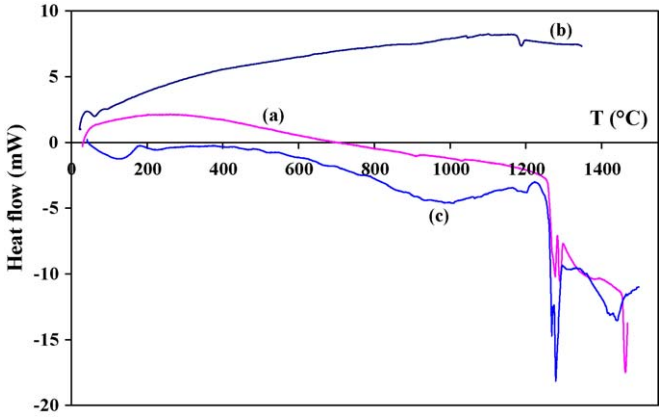

Fig. 4. DTA curves of (a) β-CTCP powder, (b) Fap powder and (c) β-CTCP–26.52 wt% Fap composites.

Fig. 4b shows the DTA curve of Fap powder, we notice the appearance of two endothermic peaks. The first peak, at 90 °C, is due to the disappearance of adsorbed water. The second peak around 1180 °C may be the result of the formation of a liquid phase occurring from binary eutectic between CaF_2 and Fap [13]. We can assume that fluorite (CaF_2) is formed as a second phase during the powder preparation of Fap.

Fig. 4c illustrates the DTA curve of CTCP–26.52 wt% Fap composites. The DTA thermogramme shows three endothermic peaks at 1268, at 1280 and at 1444 °C, which are two peaks related with two allotropic transformations of tricalcium phosphate (at 1280 °C and at 1444 °C). The temperatures of

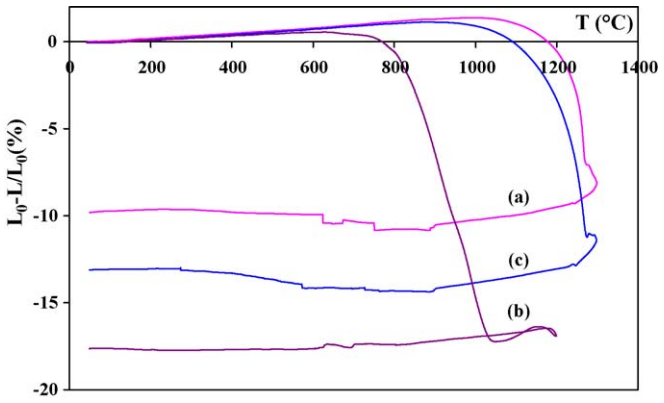

Fig. 5. Linear shrinkage versus temperature of (a) β-CTCP powder, (b) Fap powder, and (c) β-CTCP–26.52 wt% Fap composites.

Table 1
Characteristics of the powders used in the study.

Compounds	T (°C)[a]	SSA (m^2/g) ± 1.0	D_{BET} (μm) ± 0.2	D_{50} (μm)[b] ± 0.2	d[c]
Fap [14]	500	29.00	0.07	6	3.19
β-CTCP	Commercial powder	0.70	2.80	5	3.07 (β)
	1000	0.72	2.70		2.86 (α)
	1100	5.88	0.30		

[a] Calcination temperature.
[b] Mean diameter.
[c] Theoretical density.

allotropic transformations have been decreased about 10 °C (1280 °C in the place 1290 °C) and 20 °C (1444 °C in the place 1464 °C) with that of the pure β-CTCP. This result has been explained probably by the Fap effect in β-CTCP matrix.

Fig. 5 shows the dilatometric measurements of a different powder (β-CTCP, Fap and composites). The sintering temperatures began at about 1180, 775 and 1100 °C for β-CTCP, Fap and CTCP–26.52 wt% Fap composites, respectively. The addition of 26.52 wt% Fap in the matrix of β-CTCP decreases the sintering temperature of the pure β-CTCP about 80 °C (Fig. 5c).

Table 1 shows the SSA, the results of calculating the average grain size D_{BET} (calculated by Eq. (1)) and the particle size distribution data (measured by granulometric repartition) for each powder used in the study (Fap and β-CTCP). The difference between the value deducted by SSA (D_{BET}) and by granulometric repartition (D_{50}) was probably due to the presence of agglomerates in the initial powder of β-CTCP and Fap. The SSA of β-CTCP increase with calcined temperatures whereas the average grain size deceases (Table 1). At 1200 °C, it is impossible to determine their SSA because the samples are already sintered. The dilatometric analysis confirms this result (Fig. 5). In fact, the study of β-CTCP dilatometric behaviour showing that shrinkage began at about 1180 °C.

3.2. Sintering and mechanical properties of commercial tricalcium phosphate (β-CTCP)

The relative density was studied when compacts were sintered between 1050 and 1400 °C for 1 h. Fig. 6a shows the typical relationship between temperature and density. The relative density increases with sintering temperature (from 1100 to 1320 °C). After reaching its maximum value of density (84%) at 1320 °C, it remains practically constant up to 1370 °C and then decreases above this temperature where it reaches 75% at 1400 °C.

The results of the β-CTCP sample's densification according to the sintering temperature are confirmed by the mechanical study. Indeed, the Brazilian test shows us that the rupture strength increased along with the increase of sintering temperature (Fig. 6b). The maximum of mechanical resistance reaches 5.3 MPa at 1350 °C (Fig. 6b). Above 1400 °C, the rupture strength decreases abruptly.

3.3. Sintering and mechanical properties of β-CTCP–26.52 wt% Fap composites

Fig. 7a illustrates the evolution of the composites densification relative to the temperature between 1100 and

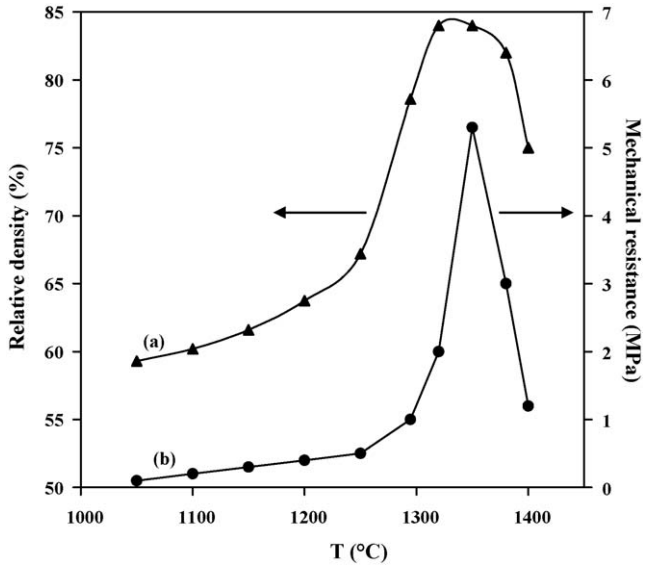

Fig. 6. Relative density and mechanical resistance versus sintering temperature of β-CTCP sintered for 1 h.

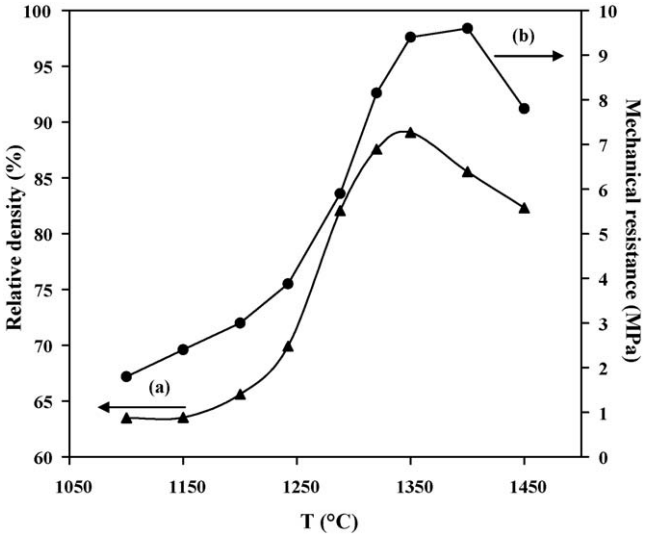

Fig. 7. Relative density and mechanical resistance versus sintering temperature of β-CTCP–26.52 wt% Fap composites sintered for 1 h.

1450 °C. The densification was variable as a function of temperature. Between 1100 and 1200 °C, the samples relative densities were very small for any samples. An increase of density was shown between 1300 and 1400 °C, where the optimum densities are about 89.1% at 1350 °C. When singly used the temperatures are similar to the densification of β-TCP [9]. But, the temperatures are relatively higher regarding those used for densification of only Fap [13,14,16]. Indeed, Fap presents a good sinterability in the temperature ranging between 900 and 1100 °C [13,14,16]. At 1450 °C, the densities decrease during the sintering process. These results were confirmed by Ben Ayed et al. during the study of elaboration and characterization of calcium phosphate biomaterial [10].

Fig. 7b shows the mechanical properties of the β-CTCP–26.52 wt% Fap composites samples according to the sintering temperature. Between 1100 and 1250 °C, the rupture strength of CTCP–26.52 wt% Fap composites samples was around 2–3 MPa. Above 1250 °C, the rupture strength increases and reaches maximum value at 1400 °C (9.6 MPa). This is attributed to the influence and effect of Fap in relative densities of the sintered composites. In fact, Fap has a good sinterability and mechanical resistance [13,14,16]. Ben Ayed et al. show that the mechanical resistance of Fap increases with temperature and reaches its maximum value about 14 MPa [16]. Above 1400 °C, the mechanical properties of composites decrease during the sintering process. Indeed, the mechanical resistance of CTCP–26.52 wt% Fap composites reaches the 8 MPa at 1450 °C.

The evolution of mechanical properties of composites was considered a function of a sintering temperature. At 1350 °C, the mechanical resistance optimum of β-CTCP sintered without Fap additive reached 5.3 MPa, whereas the resistance increases to 9.4 MPa with 26.52 wt% Fap. It is obvious that the properties of the β-CTCP and CTCP–26.52 wt% Fap composites depend directly on the properties of the departure powder (granulometric, crystallinity of the powder, chemical composition, origin of powder) and on the operative conditions of the sintering process (temperature, heating time, cycle of sintering, atmosphere) [9]. Each of these parameters has a direct effect on the final properties of the composite.

3.4. Characterization of samples after the sintering process

After the sintering process, the characteristics of the samples were investigated, using X-ray diffraction, scanning electronic microscopy, infrared spectroscopy and by analysis using ^{31}P nuclear magnetic resonance.

The XRD patterns of the β-CTCP as sintered at various temperatures (1100 and 1400 °C) for 1 h were shown in Fig. 8. All the diffraction peaks correspond to β-CTCP when the samples were sintered at 1100 °C (Fig. 8a). This spectre is identical to that one of the initial powder (β-CTCP). When the specimen were sintered at 1400 °C, we have seen low intensity peaks of α-CTCP phase (ICDD data file no. 09-0348) (Fig. 8b). This phase is a proof of the fragility of samples after the sintering process because of the different absolute densities of β-CTCP and α-CTCP (Table 1).

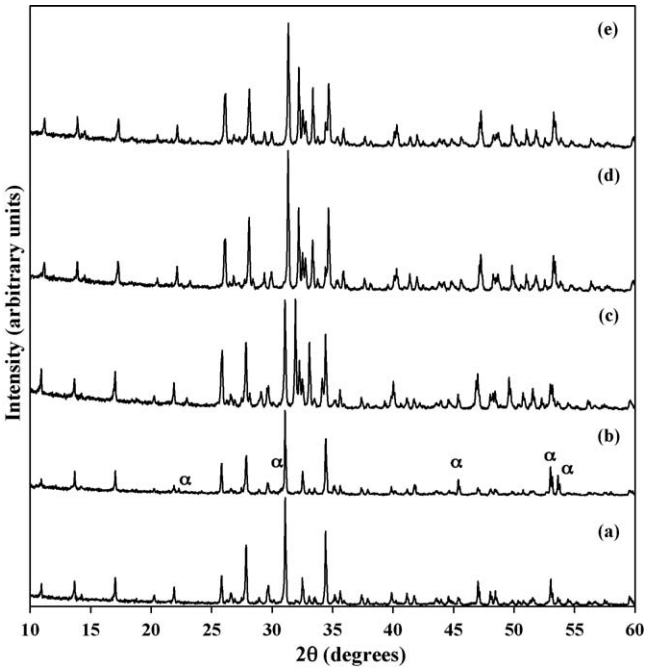

Fig. 8. XRD patterns for β-CTCP sintered for 1 h at (a) 1100 °C, (b) 1400 °C, (c) 1100 °C with 26.52 wt% Fap, (d) 1300 °C with 26.52 wt% Fap, and (e) 1400 °C with 26.52 wt% Fap (α: α-CTCP).

The XRD patterns of the CTCP–26.52 wt% Fap composites are sintered at various temperatures (1100, 1300 and 1400 °C) for 1 h were shown in Fig. 8c–e. These spectres are identical to the initial powder (β-CTCP and Fap). We conclude that β-CTCP and the Fap are steady during the sintering process and Fap prevents the formation of α-CTCP at 1400 °C. The XRD revealed only phases of departure (Fig. 8c–e). Thus, the incorporation of Fap in β-CTCP does not fulfil its right decomposition.

Fig. 9 shows the ^{31}P MAS-NMR spectra of the β-CTCP sintered for 1 h at 1100, 1300 and 1400 °C (Fig. 9a–c). All curves show that we have three environments of phosphorus. In fact, the crystal structure of β-CTCP can be described by three positions of phosphorus in the PO_4^{3-} group, running along the *c*-axis [22]. The first peak at 4.55 ppm is relative to the first position of phosphorus P(1). The second and the third peaks, at 1.10 and 0.17 ppm, are relative to the P(2) and P(3) of PO_4^{3-} group [22]. These environments are assigned to the phosphorus of Q^1 type. Otherwise, the presence of peaks (at −7.51 and −10.26 ppm) at various temperatures confirms the existence of pyrophosphate and polyphosphate (Fig. 9a–c) [23].

The Nuclear magnetic resonance chemical shift spectra of the ^{31}P of the β-CTCP–26.52 wt% Fap composites as sintered at various temperatures (1100, 1300 and 1400 °C) for 1 h are shown in Fig. 9d–f. The ^{31}P MAS-NMR solid spectra of composites show the presence of tetrahedral environment of the phosphorus. ^{31}P RMN-MAS show a single peak for Fap (at 2.8 ppm) and three peaks for β-CTCP (at 4.55, 1.1 and 0.17 ppm). The ^{31}P MAS-NMR analysis reveals the presence of three tetrahedral P sites for the β-CTCP whereas the Fap possesses only one. This result was confirmed by Yashima et al. [22]. At various temperatures, the peaks of pyrophosphate were

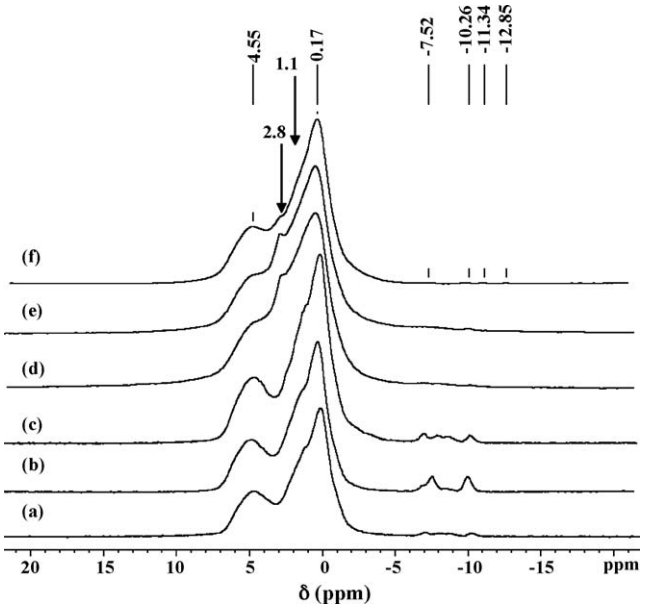

Fig. 9. ^{31}P MAS-NMR spectra of β-CTCP sintered for 1 h at (a) 1100 °C, (b) 1300 °C, (c) 1400 °C, (d) 1100 °C with 26.52 wt% Fap, (e) 1300 °C with 26.52 wt% Fap, and (f) 1400 °C with 26.52 wt% Fap.

dispaired when the β-CTCP sintered with 26.52 wt% Fap (Fig. 9d and e). The effect of Fap in the β-CTCP matrix was observed in the NMR-MAS analysis. This result confirmed the DTA and dilatometry analysis.

Fig. 10 shows SEM micrographs of the β-CTCP (fracture surfaces) sintered for 1 h at various temperatures (1100, 1250, 1300 and 1400 °C). Fig. 10a shows that at 1100 °C, the sample presents an important intergranular porosity. The continuous phases increase with the sintering temperature; β-CTCP particles went through the stages of partial coalescence (1250 °C) and full coalescence from 1300 °C, continuous phases at 1400 °C (Fig. 10b–d). A dense bioceramic was clearly formed: dense contacts between the grains and well-formed grain boundary zone. In addition the formed spherical pores prove that a liquid phase was formed at 1300 °C (Fig. 10c). The liquid phase corresponds to the binary peritectic between β-CTCP and pyrophosphate [7]. At 1400 °C, the densification was hindered and the grains growth in presence of advanced open and closed pores (Fig. 10d). The SEM observation confirms the higher porosity in the β-CTCP samples. Those originated from the micro-crack formed by small expansion in the samples at the temperature of phase transformation attributed to the low density of α-TCP (2.86 g/cm^3) than that of β-TCP (3.07 g/cm^3) (Fig. 10c and d). But also from the allotropic transformation from β to α and from α to α′.

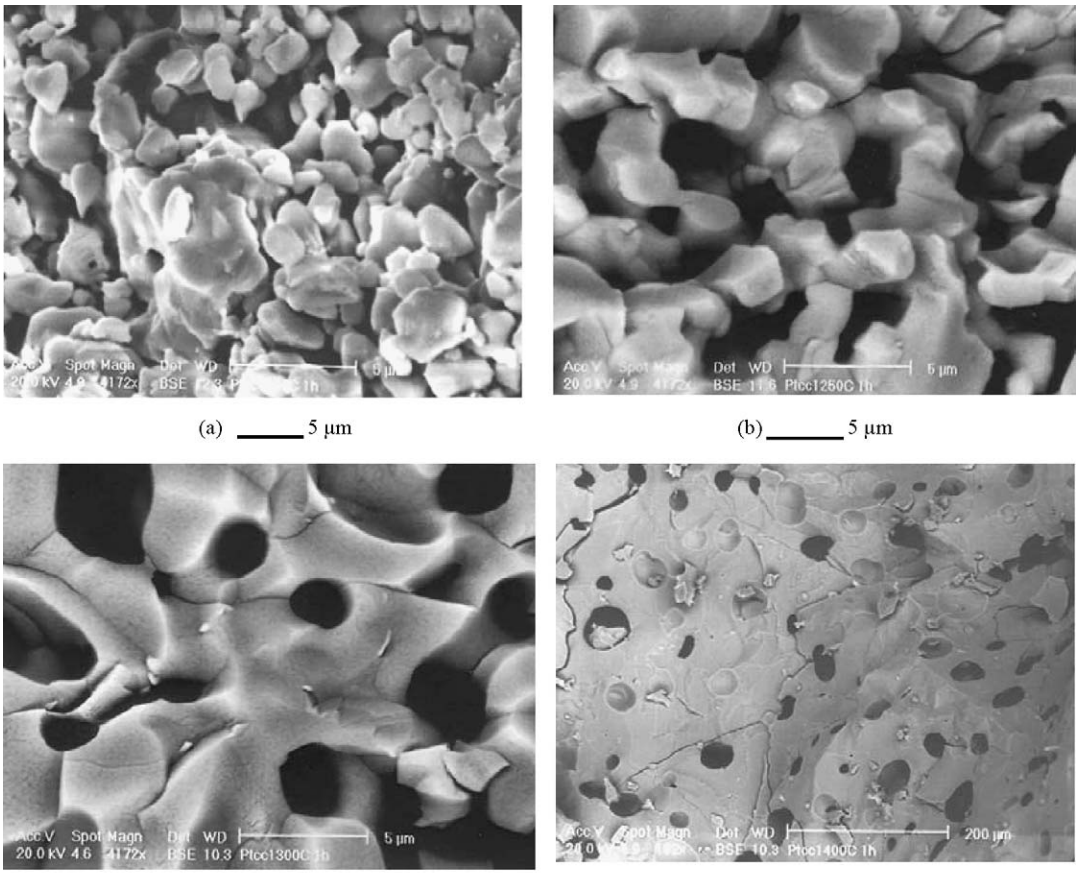

Fig. 10. SEM micrographic of β-CTCP sintered for 1 h at (a) 1100 °C, (b) 1250 °C, (c) 1300 °C, and (d) 1400 °C.

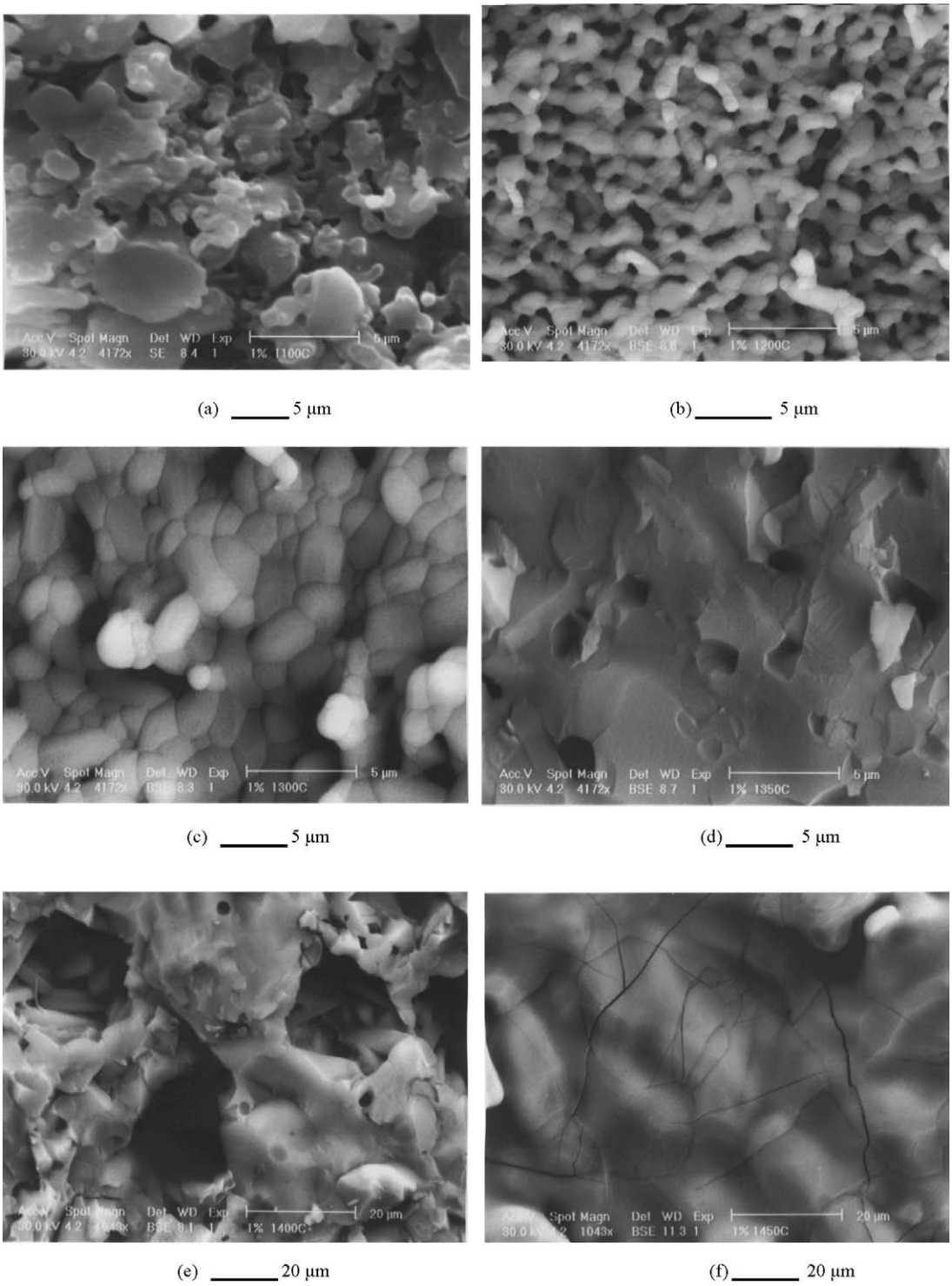

Fig. 11. SEM micrographic of β-CTCP–26.52 wt% Fap composites sintered for 1 h at (a) 1100 °C, (b) 1200 °C, (c) 1300 °C, (d) 1350 °C, (e) 1400 °C, and (f) 1450 °C.

In Fig. 11, the fracture surfaces show clearly the β-CTCP–26.52 wt% Fap composite as sintered for 1 h at various temperatures (1100, 1200, 1300, 1350, 1400 and 1450 °C) revealing the influence of the temperature of microstructural developments during the sintering process. These effects increased along the sintering temperature. The results of microstructural investigations of CTCP–26.52 wt% Fap composites show that the morphology of the samples was completely transformed (Fig. 11a–f). At 1100 °C and at 1200 °C, the sample presents an important intergranular porosity (Fig. 11a and b). At 1300 °C, the SEM micrographs of samples show liquid phase relative to the binary peritectic between pyrophosphate with the tricalcium phosphate (Fig. 11c) [7]. At 1350 °C, one notices a partial reduction of

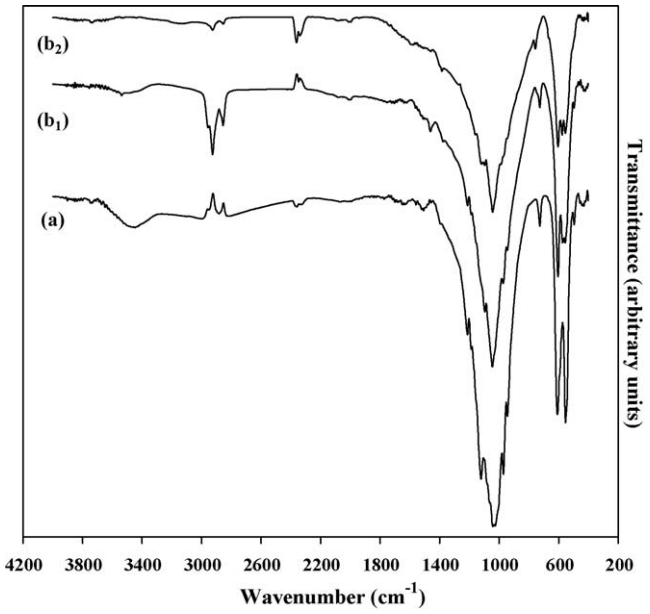

Fig. 12. IR spectra of (a) β-CTCP powder, and (b) β-CTCP sintered for 1 h with 26.52 wt% Fap at (b_1) 1300 °C, and (b_2) 1400 °C.

the porosity (Fig. 11d). At higher temperatures (1400–1450 °C), the densification is hindered by the formation of both large pores and many cracks (Fig. 10g and h). During the sintering of Fap and TCP–Fap composites, Ben Ayed et al. also observed the formation of large pores at these temperatures [10,13,14,16–18]. They are attributed to the hydrolysis of Fap and CaF_2, as expressed by the following equation:

$$CaF_{2(s)} + H_2O_{(g)} \rightarrow CaO_{(s)} + 2HF_{(g)} \quad (4)$$

$$Ca_{10}(PO_4)_6F_{2(s)} + xH_2O_{(g)} \rightarrow Ca_{10}(PO_4)_6F_{2-x}(OH)_{x(s)} + xHF_{(g)} \quad (5)$$

At higher temperatures, the composites densification and mechanical properties were hindered by the exaggerated grains growth, the effect of the allotropic transformation of tricalcium phosphate and the formation of both intragranular porosity and many cracks. The SEM micrograph illustrated the change of microstructure above 1400 °C. These results were confirmed in [10].

Fig. 12 illustrates the FT-IR spectroscopic analysis it is also performed in β-CTCP–26.52 wt% Fap composites sintered for 1 h at various temperatures (1300 and 1400 °C). Most of bands were characteristic of phosphate group of β-CTCP and Fap (at 540–600 cm^{-1} and 920–1120 cm^{-1}). The bands at 3500 cm^{-1} were assigned to the adsorbed water molecule. The intensity of pyrophosphate band at 722 cm^{-1} decreases with sintering temperature (1300–1400 °C) (Fig. 12b_1 and b_2). This result confirms the interaction between pyrophosphate with the tricalcium phosphate above 1278 °C [7].

The obtained results show that CTCP–26.52 wt% Fap composites present a good aptitude for sintering in the temperature range 1300–1400 °C. At 1350 °C, the densification was about 89.1%, whereas, the composites mechanical resistance reaches 9.6 MPa at 1400 °C. These results were confirmed with those obtained in [6–10]. Above 1400 °C, the densification and the mechanical resistance of β-CTCP and β-CTCP–26.52 wt% Fap composites have been hindered by grain growth, allotropic transformation and the formation of an important intragranular porosity. Indeed, many studies of the β-TCP and TCP–Fap composites prove that the allotropic phase transformations are related to the sintered temperature [6–10].

The preliminary results obtained in this study have shown that the Fap has a potential to be further developed into an alternative system to produce denser β-CTCP bodies. Further investigations are still under way to investigate the influence of Fap on the densification, microstructure and mechanical properties of β-CTCP–26.52 wt% Fap composites bioceramic.

4. Conclusion

The effect of fluorapatite additive in tricalcium phosphate matrix was observed in different thermal analyses, dilatometry analysis and ^{31}P RMN-MAS analysis. The effect of Fap additive (26.52 wt%) in β-CTCP matrix was studied during the sintering process. This survey allowed us to define the sintering temperature for which CTCP–26.52 wt% Fap composites should have an optimal densification and a best mechanical resistance. The composites present the best properties when composites were sintered between 1300 and 1400 °C. The densification reaches 89.1% when sintered at 1350 °C for 1 h as heating temperature. At 1350 °C, the mechanical resistance of β-CTCP sintered without Fap additives was about 5.3 MPa, whereas, the resistance increases to 9.4 MPa for β-CTCP sintered with 26.52 wt% Fap. This result is due to the dense microstructure of sintered Fap samples. Above 1400 °C, the densification and mechanical properties were hindered by grain growth and the formation of intragranular porosity.

References

[1] L.L. Hench, Bioceramics: from concept to clinic, J. Am. Ceram. Soc. 74 (7) (1991) 1487–1510.
[2] P. Uwe, E. Angela, R. Christian, A pyrolytic route for the formation of Hydroxyapatite–fluorapatite solid solutions, J. Mater. Sci.: Mater. Med. 4 (3) (1993) 292–295.
[3] J.C. Elliott, Structure and Chemistry of the Apatite and Other Calcium Orthophosphates, Elsevier Science B.V., Amsterdam, 1994.
[4] J. Hemmerle, A. Oncag, S. Erturk, Ultrastructural features of the bone response to a plasma-sprayed hydroxyapatite coating in sheep, J. Biomed. Mater. Res. 36 (1997) 418–425.
[5] E. Landi, A. Tampieri, G. Celotti, S. Sprio, Densification behaviour and mechanisms of synthetic hydroxyapatites, J. Eur. Ceram. Soc. 20 (2000) 2377–2387.
[6] H.K. Varma, S. Sureshbabu, Oriented growth of surface grains in sintered β tricalcium phosphate bioceramics, Mater. Lett. 49 (2001) 83–85.
[7] A. Destainville, E. Champion, D. Bernache-Assolant, E. Labore, Synthesis, characterization and thermal behaviour of apatitic tricalcium phosphate, Mater. Chem. Phys. 80 (2003) 69–77.
[8] C.X. Wang, X. Zhou, M. Wang, Influence of sintering temperatures on hardness and Young's modulus of tricalcium phosphate bioceramic by nanoindentation technique, Mater. Characterization 52 (2004) 301–307.
[9] F. Ben Ayed, K. Chaari, J. Bouaziz, K. Bouzouita, Frittage du phosphate tricalcique, C. R. Phys. 7 (7) (2006) 825–835.
[10] F. Ben Ayed, J. Bouaziz, Elaboration et caractérisation d'un biomatériau à base de phosphate de calcium, C. R. Phys. 8 (1) (2007) 101–108.

[11] E.D. Franz, R. Telle, Reaction hot pressing fluorapatite for dental implants, in: P. Vincenzini (Ed.), High Tech. Ceram., Elsevier Sciences Publishers, B.V., Amsterdam, 1987, p. 31.
[12] F. Mark, P.W. Brown, Low-temperature formation of fluorapatite in aqueous solution, J. Am. Ceram. Soc. 75 (12) (1992) 401–407.
[13] F. Ben Ayed, J. Bouaziz, K. Bouzouita, Pressureless sintering of fluorapatite under oxygen atmosphere, J. Eur. Ceram. Soc. 20 (8) (2000) 1069–1076.
[14] F. Ben Ayed, J. Bouaziz, K. Bouzouita, Calcination and sintering of fluorapatite under argon atmosphere, J. Alloys Compd. 322 (1–2) (2001) 238–245.
[15] F. Ben Ayed, J. Bouaziz, I. Khattech, K. Bouzouita, Produit de solubilité apparent de la fluorapatite frittée, Ann. Chim. Sci. Mater. 26 (6) (2001) 75–86.
[16] F. Ben Ayed, J. Bouaziz, K. Bouzouita, Résistance mécanique de la fluorapatite frittée, Ann. Chim. Sci. Mater. 31 (4) (2006) 393–406.
[17] F. Ben Ayed, J. Bouaziz, Sintering of tricalcium phosphate–fluorapatite composites by addition of alumina, Ceram. Int. 34 (8) (2008) 1885–1892.
[18] F. Ben Ayed, J. Bouaziz, Sintering of tricalcium phosphate–fluorapatite composites with zirconia, J. Eur. Ceram. Soc. 28 (2008) 1995–2002.
[19] S. Brunauer, P.H. Emmet, J. Teller, Adsorption of gases in multimolecular layers, J. Am. Chem. Soc. 60 (1938) 310–319.
[20] ISRM, Suggested methods for determining tensile strength of rock materials, Int. J. Rock Mech. Min. Sci. Geomech. Abstr. 15 (1978) 99–103.
[21] ASTM C496. Standard test method for splitting tensile strength of cylindrical concrete specimens, Annual Book of ASTM, Standards, vol. 0.042, ASTM, Philadelphia, 1984, pp. 336–341.
[22] M. Yashima, A. Sakai, T. Kamiyama, A. Hoshikawa, Crystal structure analysis of β-tricalcium phosphate $Ca_3(PO_4)_2$ by neutron powder diffraction, J. Solid State Chem. 175 (2003) 272–277.
[23] B. Moreno, B.N. Bailey, S. Luo, M.B. Martin, M. Kuhlenschmidt, S.N.J. Moreno, R. Docampo, E. Oldfield, Biochem. Biophys. Res. Commun. 284 (2001) 632–637.